

BH3-only protein Bmf mediates apoptosis upon inhibition of CAP-dependent protein synthesis

F Grespi¹, C Soratroi¹, G Krumschnabel¹, B Sohm¹, C Ploner², S Geley², L Hengst³, G Häcker⁴ and A Villunger^{*1}

Tight transcriptional regulation, alternative splicing and/or post-translational modifications of BH3-only proteins fine-tune their proapoptotic function. In this study, we characterize the gene locus of the BH3-only protein Bmf (Bcl-2-modifying factor) and describe the generation of two major isoforms from a common transcript in which initiation of protein synthesis involves leucine-coding CUG. Bmf_{CUG} and the originally described isoform, Bmf-short, display comparable binding affinities to prosurvival Bcl-2 family members, localize preferentially to the outer mitochondrial membrane and induce rapid Bcl-2-blockable apoptosis. Notably, endogenous Bmf expression is induced on forms of cell stress known to cause repression of the CAP-dependent translation machinery such as serum deprivation, hypoxia, inhibition of the PI3K/AKT pathway or mTOR, as well as direct pharmacological inhibition of the eukaryotic translation initiation factor eIF-4E. Knock down or deletion of Bmf reduces apoptosis under some of these conditions, demonstrating that Bmf can act as a sentinel for stress-impaired CAP-dependent protein translation machinery.

Cell Death and Differentiation (2010) 17, 1672–1683; doi:10.1038/cdd.2010.97; published online 13 August 2010

The Bcl-2 family comprises a number of cell death- and survival-promoting proteins that are characterized by structural motives, known as Bcl-2 homology (BH) domains. Prosurvival family members such as Bcl-2 itself, Bcl-xL, Bcl-w or Mcl-1 contain up to four homology domains (BH1–4), whereas proapoptotic members of the same family either possess three out of four BH domains, for example, Bax and Bak (BH123 proteins) or only the BH3 domain, such as Bim, Bid, Bad or Bmf, referred to as BH3-only proteins. Biochemical evidence suggests that BH3-only proteins can interact with and antagonize partially overlapping subsets of Bcl-2 homologs, allowing oligomerization of Bax or Bak, subsequent destabilization of mitochondrial integrity, caspase activation and cell death. In an alternative model, some BH3-only proteins such as Bim or Bid are proposed to interact directly with Bax/Bak-like molecules for apoptosis induction.¹

The role of BH3-only proteins in normal physiology has been addressed primarily by analyzing mouse models lacking individual genes. Loss of Puma protects neurons, primary lymphocytes, myeloid cells and mouse embryonic fibroblast (MEF) not only from DNA damage-induced apoptosis but also from certain p53-independent cell death stimuli, such as glucocorticoids or serum deprivation, whereas Noxa seems to have a more restricted role in mediating DNA damage responses.^{2,3} The absence of Bid prevents liver failure in response to FAS ligation, confirming the role of Bid as the connecting element between extrinsic and intrinsic cell death pathways.^{4,5} Loss of Bim causes lymphadenopathy and

subsequent autoimmunity mainly due to negative selection defects⁶ and acts as a suppressor of *c-myc*-driven lymphomagenesis.⁷

Little is known about the biology of Bmf that seems to be regulated in a manner similar to Bim. Both molecules share a highly conserved dynein light chain (DLC)-binding motif near their N termini that can target Bmf to the actin cytoskeleton and Bim to microtubules.⁸ Bmf can be released from the cytoskeleton in response to UV radiation or during detachment-induced apoptosis (anoikis), which prevents epithelial cells from colonizing elsewhere.⁹ However, both forms of cell death proceed normally in MEFs and/or gastrointestinal epithelial cells from *bmf*^{-/-} mice,¹⁰ suggesting redundancy with other BH3-only proteins. In hemopoietic cells, Bmf is widely expressed and has been implicated in cytokine withdrawal-induced apoptosis of granulocytes in which the protein was reported to accumulate during *in vitro* culture.¹¹ Multiple isoforms can be detected in lymphocytes and hence alternative splicing of *bmf* may also contribute to regulate its *in vivo* function.¹⁰ Two splice variants, namely BMF II and BMF III, are expressed in normal and malignant human B cells, derived from patients with B-cell chronic lymphocytic leukemia (B-CLL). Surprisingly, these novel variants lack a functional BH3 domain and BMF III also contains a different carboxy terminus. Overexpression in HeLa cells increased their colony-forming potential, whereas BMF I, as previously reported, showed proapoptotic activity.¹² B-CLL cells undergo rapid apoptosis *in vitro* and this cell death correlated with

¹Division of Developmental Immunology, Innsbruck Medical University, Biocenter, Innsbruck, Austria; ²Division of Molecular Pathophysiology, Innsbruck Medical University, Biocenter, Innsbruck, Austria; ³Division of Medical Biochemistry, Innsbruck Medical University, Biocenter, Innsbruck, Austria and ⁴Institute for Medical Microbiology and Hygiene, Universität Freiburg, Freiburg, Germany

*Corresponding author: A Villunger, Division of Developmental Immunology, Biocenter, University of Innsbruck, A-6020 Innsbruck, Austria.

Tel: +43 51 290 037 0380; Fax: +43 51 290 037 3960; E-mail: andreas.villunger@i-med.ac.at

Keywords: apoptosis; Bcl-2 family; BH3-only proteins; Bmf

Abbreviations: Bmf, Bcl-2-modifying factor; BH, Bcl-2 homology domain; IVT, *in vitro* transcription; IVTT, *in vitro* transcription and translation; TSS, transcription start site; IRES, intra-ribosomal entry site; FF, Firefly; RN, Renilla; ECFP, enhanced cyan fluorescent protein; SV, Simian virus; MEF, mouse embryonic fibroblast; sh, short hairpin; ORF, open reading frame; eIF, eukaryotic initiation factor; DLC, dynein light chain

Received 31.3.10; revised 24.6.10; accepted 05.7.10; Edited by C Borner; published online 13.8.10

enhanced mRNA expression of BMF1.¹² Consistently, genetic ablation of all Bmf isoforms expressed in mice showed not only a role in the regulation of normal B-cell homeostasis but also irradiation-driven,¹⁰ as well as oncogene-driven tumorigenesis.¹³ Finally, a role for Bmf in necroptotic cell death in L929 fibroblasts was reported, but its exact role in this process remains to be fully understood.¹⁴

In this study, we characterize the *bmf* gene locus in detail, report the molecular basis of the generation of the two major isoforms of Bmf, designated as Bmf-short (Bmf_S) and Bmf_{CUG}, as well as provide evidence that Bmf can act as a sensor for stress that associates with the repression of the conventional CAP-dependent translation machinery.

Results

An additional conserved translation start site in the *bmf* mRNA sequence allows expression of a longer Bmf isoform, Bmf_{CUG}. Analysis of intron–exon boundaries in the mouse *bmf* locus showed a possible alternative start codon only 4 base pairs upstream of the 5' end of the longest cDNA clone that was originally identified as a putative additional transcription start site (TSS) (Figure 1a). Inclusion of this 5' sequence indicated that the mouse *bmf* mRNA sequence

(4.8 kb in size) now contained a significantly longer open reading frame (ORF) (816 bp) as that initially described (558 bp).¹⁵ Translation *in silicio* predicted a longer version of the mouse Bmf protein, designated herein as Bmf-long (Bmf_L), with an alternative extended N terminus, ~30 kDa in size, but otherwise identical to the originally published protein sequence, referred to as Bmf_S.

Screening of EST databases confirmed that transcripts containing this upstream ATG can be found in cDNA libraries, for example, derived from mouse E13 embryonic heart muscle tissue or E12 mouse ovary, suggesting that this longer ORF may be used *in vivo* to generate Bmf_L. Consistently, two major isoforms of Bmf are found by western analysis in lymphocyte extracts from adult mice¹⁰ or human leukemia cells¹⁶ and cell lines.¹⁷ Immunoprecipitation using Bmf-specific antibodies and subsequent immunoblotting showed that two protein products were precipitated from mouse splenocytes (Figure 1b). The smaller product, migrating at ~22 kDa, presumably represented the originally described mBmf_S isoform, as indicated by comparison with mBmf_S transiently expressed in 293T cells (Figure 1b). The slower migrating band was ~26 kDa in size and we initially considered it to represent Bmf_L. Interestingly, two additional bands were detected in lysates and IP complexes from

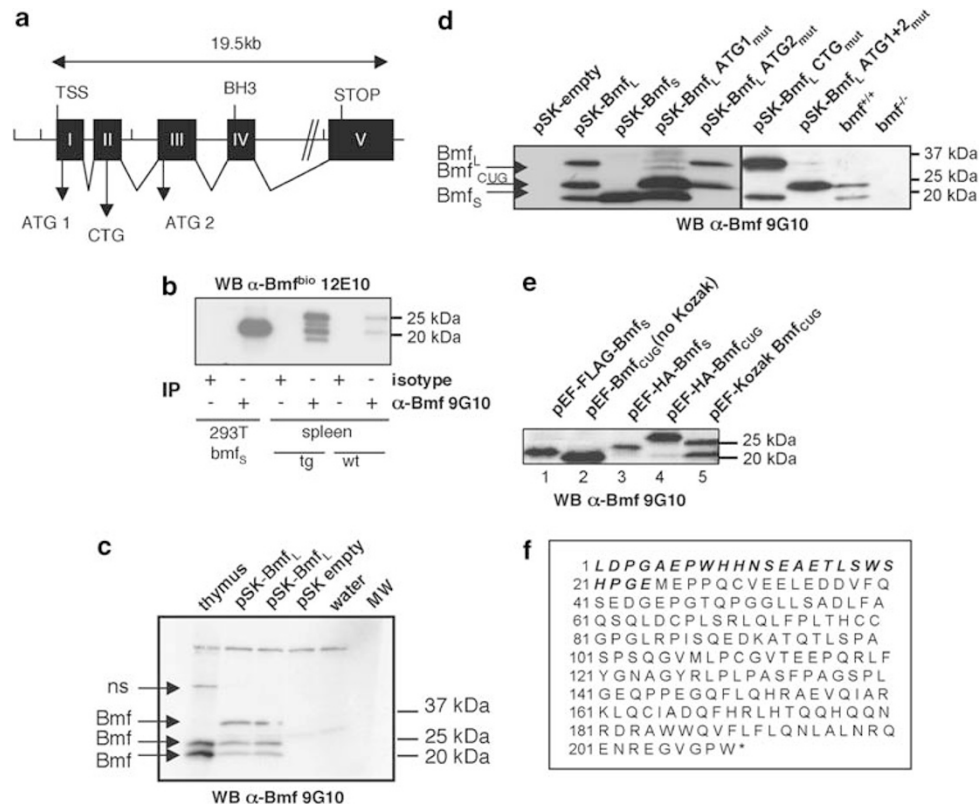


Figure 1 Characterization of Bmf isoforms. (a) Schematic representation of the mouse *bmf* gene locus located on chromosome 2 (not to scale). ATGs that may be used for translation initiation are located in exons 1 and 3. A Kozak-flanked CTG can be found in exon 2. (b) Bmf was immunoprecipitated using rat anti-Bmf 9G10 mAb from 293T cells transiently transfected with an expression plasmid encoding Bmf_S cDNA or splenocytes from wild-type (wt) or *vav-bcl-2* transgenic (tg) mice. Immunoblotting was performed using biotinylated rat anti-Bmf-specific mAb (12E10). (c) Bmf_L cDNA in pSKblue was used in a coupled *in vitro* transcription translation reaction. IVTT reactions were separated by SDS-PAGE before immunoblotting (ns = nonspecific). (d) IVTT reactions of Bmf_L and different mutated versions were separated by SDS-PAGE and immunoblotted using anti-Bmf antibody. Thymic cell extracts from wt and *bmf*^{-/-} mice served as controls. (e) Expression of different versions of epitope-tagged or epitope-untagged Bmf isoforms in transiently transfected 293T cells. (f) Amino acid sequence of mouse Bmf_{CUG}/Bmf_S. Amino acids specific for Bmf_{CUG} are shown in bold italic

Bcl-2-overexpressing lymphocytes (Figure 1b, Supplementary Figure 1a and b), 24 and 20 kDa in size, which are absent or only poorly expressed in most wild-type (wt) lymphocyte subsets analyzed.¹⁰ These proteins may represent either low-abundance splice variants of *bmf*, post-translationally modified versions or degradation products of the two major isoforms (see below). Phosphatase treatment of cell lysates excluded phosphorylation as a possible modification (Supplementary Figure 1a). Taken together, these observations suggest that (co)-transcriptional modifications such as differential splicing, alternative promoter and/or start-site usage or other post-translational modifications account for the generation of multiple Bmf isoforms.

To verify that both putative start sites contained in the *mbmf* mRNA can be used, we generated and subcloned a cDNA encoding the ORF for Bmf_L into pSK bluescript and performed a T7-driven coupled *in vitro* transcription/translation reaction (IVTT) in rabbit reticulocyte lysates in the presence or absence of ³⁵S-methionine. The reaction products were separated by SDS-PAGE, exposed to X-ray film or subjected to immunoblotting using an anti-Bmf-specific mAb. Three major protein products of comparable size were detected by both methods (Figure 1c and d, not shown). Notably, two of those products migrated with the same behavior patterns as those recognized in lysates from mouse thymocytes. However, the longest product generated by IVTT did not seem to have an endogenous counterpart (Figure 1c). Mutation of the second, internal ATG2 led to the disappearance of the shortest Bmf product, indicating that only Bmf_S is translated from this internal ATG in exon 3 and excluding the possibility that the other two products may arise from post-translational modification of Bmf_S (Figure 1d). In contrast, deletion of the first ATG1 led to the disappearance of the largest protein product but the two other products, resembling the endogenous proteins in size were still produced. As there was no other ATG in frame with the ORF of Bmf_S, we searched for the presence of alternative start sites and discovered a CTG, which was flanked by a strong Kozak sequence in frame with the downstream ATG2 that gives rise to Bmf_S. Site-directed mutagenesis confirmed that this CTG is recognized efficiently by the translation machinery and can be used to generate a longer isoform of Bmf, designated herein as Bmf_{CUG}, still produced when both ATGs in the cDNA were mutated (Figure 1d). Overexpression of a single transcript containing this putative translation initiating CTG in the context of the surrounding Kozak sequence in 293T cells allowed efficient coexpression of Bmf_{CUG} and Bmf_S (lane 5), whereas in its absence, only Bmf_S was translated into the protein (lane 2) (Figure 1e). Epitope tagging allowed for the efficient expression of Bmf_S or Bmf_{CUG} individually (lanes 3 and 4). We concluded that these two protein products most likely represent the endogenous proteins recognized by our anti-Bmf antibodies in hemopoietic cells or after IVTT (Figure 1b and d). Sequence alignment showed that this CTG site was conserved across all mammalian species in which genomic DNA of this region was contained in the *Ensemble* database (Figure 2), allowing for translation of Bmf_{CUG}, containing 24 additional amino acids (aa) at its N terminus (Figure 1f). In contrast, the first ATG found in exon I was either not present as in horse (*equus*) or, in other species such as humans and

chimpanzee, this ATG1 was not in frame with the downstream ATG2, used to translate Bmf_S (Figure 2).

Bmf_{CUG} and Bmf_S bind the same Bcl-2 family proteins and show comparable apoptotic potential, as well as subcellular localization. Constructs that allow expression of either isoform alone (not shown) or both isoforms at the same time (Figure 1e) were transiently transfected together with FLAG-tagged versions of Bcl-2, Bcl-xL, Bcl-w, Mcl-1 or the viral Bcl-2 homologs, BHRF1 and KS-Bcl-2 (Figure 3a). Coimmunoprecipitation analysis showed that both isoforms effectively interacted with all mammalian prosurvival proteins tested, but not with their viral counterparts (Figure 3b). As expected, introduction of a leucine to alanine mutation in the BH3 domain (L/A) abrogated interaction with Bcl-2, but we repeatedly observed residual binding of both Bmf isoforms to Mcl-1 (Figure 3b).

To assess possible differences in their proapoptotic potential, we generated IL3-dependent BaF3 cells that stably expressed the above-mentioned prosurvival Bcl-2 family proteins alone or together with one or the other isoforms of Bmf. Upon IL3-deprivation, BaF3 cells undergo rapid cell death that can be blocked by overexpression of antiapoptotic Bcl-2 proteins (Supplementary Figure 2a), unless these are themselves blocked by BH3-only proteins.¹⁵ In line with their ability to bind to Bcl-2, Bcl-xL or Mcl-1 in our IP analysis, Bmf_{CUG} or Bmf_S antagonized the prosurvival effect of these Bcl-2 family members upon IL3 deprivation (Supplementary Figure 2). Bmf overexpression failed to antagonize the antiapoptotic effect of the two viral Bcl-2-like proteins, consistent with a lack of direct interaction in our IP analysis (Figure 3b). Notably, BaF3 cells coexpressing Bcl-w together with Bmf_S or Bmf_{CUG} resisted apoptosis upon IL3 deprivation (Supplementary Figure 2), which may have been due to extremely high levels of transgenic Bcl-w, which, presumably, were not neutralized effectively by overexpressed Bmf (not shown).

To extend our observations to a different model system, we performed lentiviral transduction of apoptosis-sensitive U2OS osteosarcoma cells with constructs encoding for Bmf_S or Bmf_{CUG}, as well as Bmf_S^{L138A} or Bmf_{CUG}^{L162A}, carrying a point mutation in the BH3 domain. Parallel transduction using a GFP-encoding virus served as a control to quantify infection efficiency (usually >90%) and treatment-related cell death (usually ~20%). Although both isoforms of Bmf induced comparable apoptotic cell death, BH3-domain mutant versions failed to do so, when compared with GFP-transduced controls (Figure 4). Seeding identical numbers of transduced U2OS cells confirmed that both isoforms of Bmf, but not its L/A-mutant versions, strongly reduced the colony-forming potential of these cells (Figure 5a). Finally, we investigated whether Bmf_{CUG} and Bmf_S would have different preferences for Bax or Bak to kill cells. Therefore, Simian virus (SV)40-MEF expressing or lacking *bak*, *bax* or both genes were transduced with the two Bmf isoforms alone or a construct that allows simultaneous expression of both proteins. As shown in Figure 5b, both isoforms reduced the colony formation of wt-, Bax- and Bak-deficient cells, suggesting that both BH123 proteins can be engaged to mediate Bmf-induced apoptosis. Bmf_S seemed to kill SV40 MEF somewhat more effectively

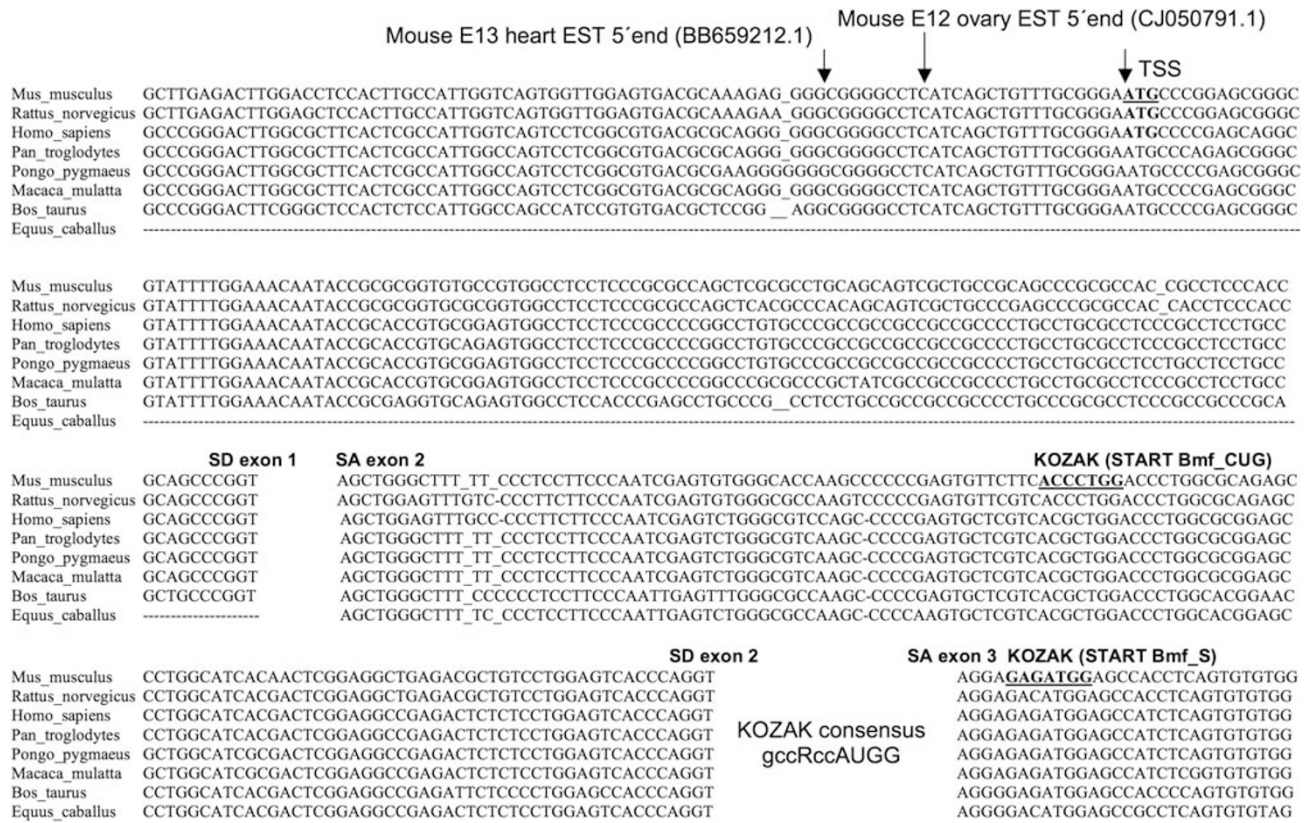


Figure 2 The non-conventional CUG-translation initiation site of Bmf is conserved among mammals. Alignment of the Bmf genomic DNA sequence derived from various mammalian species. All but *equus* contain the conserved exon 1 encoding predicted transcription start sites (TSS), marked by arrows. All available mammalian Ensemble sequences contain exon 2 with the Kozak-flanked CTG and the originally defined ATG translation start site in exon 3. Arrows indicate putative transcription start sites found in ESTs from the embryonic ovary and heart tissue. SA = splice acceptor, SD = splice donor site

and preferentially in a Bax-dependent manner. Notably, *bax*^{-/-}*bak*^{-/-} MEF, despite being highly resistant to the effects of etoposide treatment, also showed reduced colony formation upon transduction with Bmf when both isoforms were expressed simultaneously (Figure 5b).

To investigate whether the additional 24 aa found in Bmf_{CUG}, predicted to contain an additional α -helix may cause differences in subcellular localization, we transiently transfected HA-tagged versions of the individual isoforms into 293T HEK cells or NIH3T3 fibroblasts, followed by immunofluorescence analysis demonstrating a predominantly mitochondrial localization (Figure 6a and not shown). As the anti-Bmf antibodies currently available are not suitable for immunofluorescence, we studied localization performing biochemical fractionation experiments. Analysis of cytoplasmic and mitochondrial fractions from NIH3T3 cells that were left untreated or incubated with cytochalasin D for 16 h, a stimulus reported to induce translocation of Bmf from the actin cytoskeleton to the mitochondria,¹⁵ confirmed that endogenous Bmf can already be found in the mitochondrial fraction in untreated cells (Figure 6b). Alkaline extraction also indicated that Bmf is not simply loosely attached to the outer mitochondrial membrane but, similar to Bim,¹⁸ must have been actively inserted into it (Figure 6b). Finally, we also investigated whether both proteins may display differences in protein stability but again, at least under steady-state

conditions, both isoforms were equally sensitive to CHX treatment showing a half-life of approximately 3–4 h, as assessed in WEHI231 pre-B cells (Supplementary Figure 1c) or NIH3T3 fibroblasts (not shown).

Bmf_{CUG} and Bmf_S can be translated in a CAP-independent manner. As non-ATG-dependent initiation often associates with translation of proteins from intra-ribosomal entry sites (IRESs),¹⁹ we speculated whether the RNA sequence between both translation start sites possesses the capacity to enable CAP-independent translation. To test this, we first subcloned different cDNA fragments encoding different portions of the 5' end of the *bmf* mRNA into a bicistronic luciferase reporter system in which a minimal SV40 promoter drives the expression of one mRNA encoding the Renilla (RN) luciferase, followed by a spacer, and the ORF encoding for the Firefly (FF) luciferase. Inserting the 258-bp TSS-ATG2 fragment or the 72 bp CTG-ATG2 fragment into this spacer region showed that the longer fragment was able to promote a significant expression of the FF reporter, whereas insertion of a nonrelated sequence from the glyceraldehyde-3-phosphate dehydrogenase (GAPDH) gene was unable to do so (Figure 7a). Finally, when the same experiment was performed using modified constructs that carry an additional stem-loop structure between the SV40 promoter

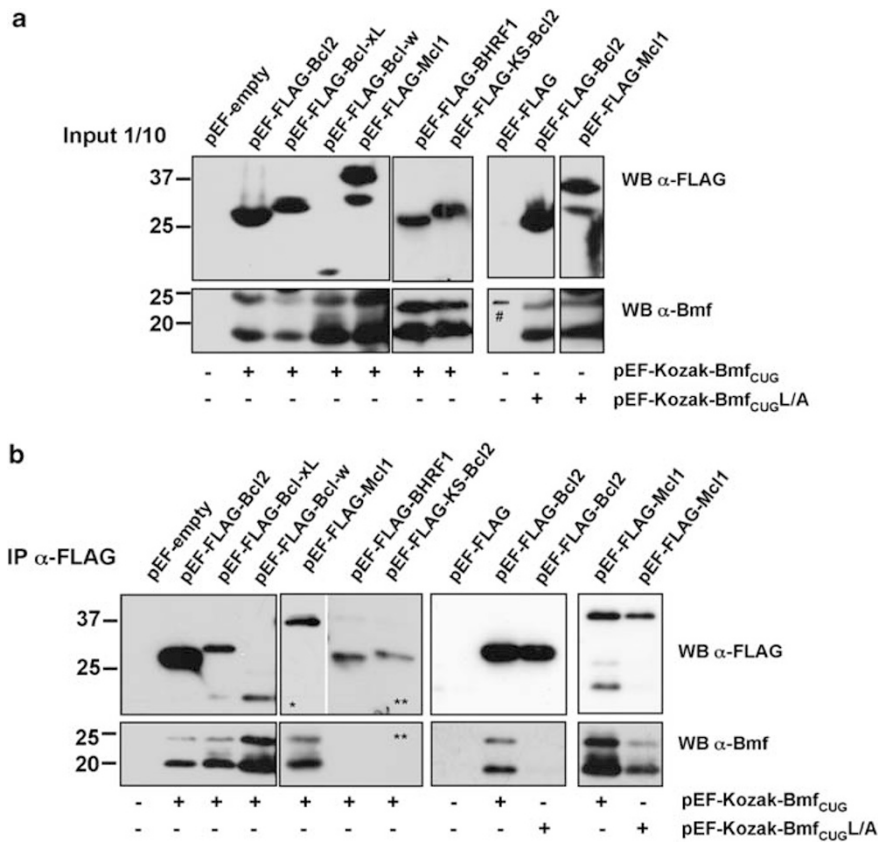


Figure 3 Bmf_S and Bmf_{CUG} show the same interaction pattern with anti-apoptotic Bcl-2 family members. (a) Bmf_S and Bmf_{CUG} were overexpressed simultaneously in 293T cells together with FLAG-tagged versions of Bcl-2, Bcl-xL, Bcl-w, Mcl-1, BHRF1 or KS-Bcl-2. Expression of the transgene-derived protein was confirmed by immunoblotting using anti-FLAG- or anti-Bmf-specific mAbs (# = marker labeling). (b) Immunoprecipitation was performed using anti-FLAG-M2 mAb. Immune complexes were separated by SDS-PAGE on 4–20% Tris-glycine gels. After electroblotting, nitrocellulose membranes were subjected to immunoblotting using the anti-Bmf mAb (17A9). Membranes were stripped and reprobed with a rat-anti-FLAG antibody. One out of three independent experiments yielding similar results is shown (* short exposure, ** long exposure)

and the ORF for RN, hindering CAP-dependent translation, a clear shift in the ratio between RN/FF was observed in the presence of the TSS-ATG2 fragment (Figure 7a). The well-described IRES element from the cyclin-dependent kinase inhibitor *p27* was used as an internal control.²⁰ To exclude residual promoter activity in the tested cDNA fragments to be responsible for the observed FF activity in our dual reporter assay, the same DNA elements were also inserted into the promoter-less pGL2luc luciferase expression vector and its activity was compared with that of a *bona fide* *bmf* promoter fragment encoding nucleotides –600 to +70 in relation to the TSS. Although the latter fragment induced significant luciferase activity upon overexpression in 293T cells, all other DNA fragments did not, thus arguing against this possibility (Figure 7b). To confirm this observation in a different experimental system, the same 258 bp fragment (TSS-ATG2), conferring expression of the FF luciferase in our dual-luciferase experiments was subcloned in between the ORFs of the two fluorescent proteins, enhanced cyan fluorescent protein (ECFP) and Venus (Supplementary Figure 3a). Fluorescence microscopy of 293T cells transfected with constructs allowing either expression of both fluorescence proteins as a single fusion protein or both ORFs separately, due to insertion of the TSS-ATG2 element

preceded by a STOP codon after ECFP, confirmed that both fluorescent proteins are translated individually in cells transfected with the latter construct (Supplementary Figure 3b). However, as we could not rule out completely that ribosomal slipping may contribute to Venus expression (or expression of the second luciferase gene in Figure 7a), we investigated whether blocking CAP-dependent translation by addition of rapamycin or the CAP-translation inhibitor 4EGI-1 favored the expression of the second fluorescent protein, Venus, over ECFP. Consistent with our idea that the 5' end of the *bmf* mRNA contains features of an IRES element, we observed a clear shift toward the expression of the second fluorescence under these conditions (Supplementary Figure 3c) that should not become visible, if both proteins were synthesized in a strictly CAP-dependent manner. Finally, we transcribed *bmf* cDNA, including a polyA tail *in vitro* without adding a 5'CAP and used this mRNA in a separate translation reaction. cDNA encoding GFP served as a control. The translation reactions were then separated by SDS-PAGE, and immunoblotting was performed using anti-Bmf-specific and anti-GFP-specific antibodies. Although *in vitro* transcription (IVT) of the GFP mRNA did not generate any detectable protein expression, due to the lack of the 5'CAP structure, we observed that Bmf_S was effectively

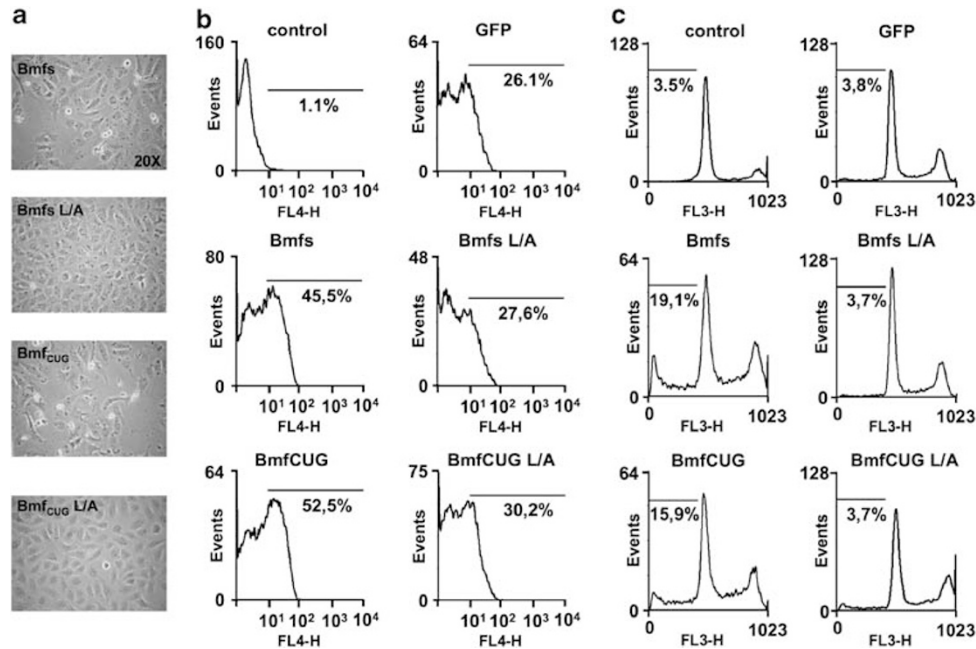


Figure 4 Bmfs and Bmf_{CUG} show similar potency in inducing apoptotic cell death. U2OS cells were transduced with lentiviruses encoding wt or inactive mutant versions (L/A) of Bmfs, Bmf_{CUG} or GFP, as a control. Twenty-four hours later, transduction efficiency was monitored by flow-cytometric analysis of the GFP-transduced cells (usually > 90% GFP⁺). Microscopic images were taken (a) and cell death was quantified by either APC-Annexin-V (b) or sub-G1-staining, (c) followed by flow-cytometric analysis. One out of three independent experiments yielding similar results is shown

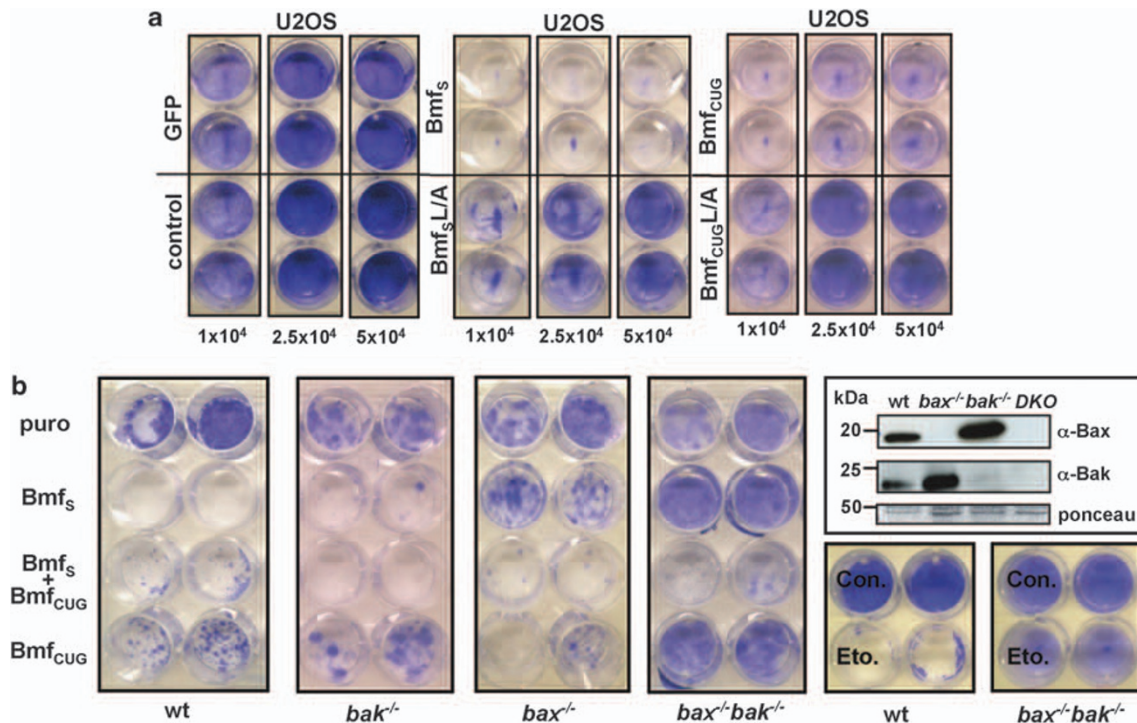


Figure 5 Bmfs and Bmf_{CUG} reduce clonal survival in U2OS cells and can engage either Bax or Bak to kill. (a) Lentivirally transduced U2OS cells were seeded in different cell numbers and cultured for additional 5 days. Surviving colonies were stained using crystal violet. One representative experiment out of two, yielding similar results is shown. (b) SV40-MEF proficient or deficient for Bax, Bak or both were transduced with a retrovirus encoding the puromycin resistance gene alone or in combination with Bmfs or Bmf_{CUG} individually, or a plasmid allowing simultaneous translation of both isoforms (Bmfs_{CUG}). MEFs were subjected to puromycin selection (2 μg/ml) for 7 days and surviving colonies were stained using crystal violet. One representative experiment out of three, yielding similar results is shown. Expression of Bax or Bak in the mutant MEF lines was monitored by western blot. MEFs expressing Bax and Bak (wt) or lacking both genes were also exposed to 1.0 μg of etoposide for 72 h or were left untreated to confirm their intrinsic apoptosis resistance

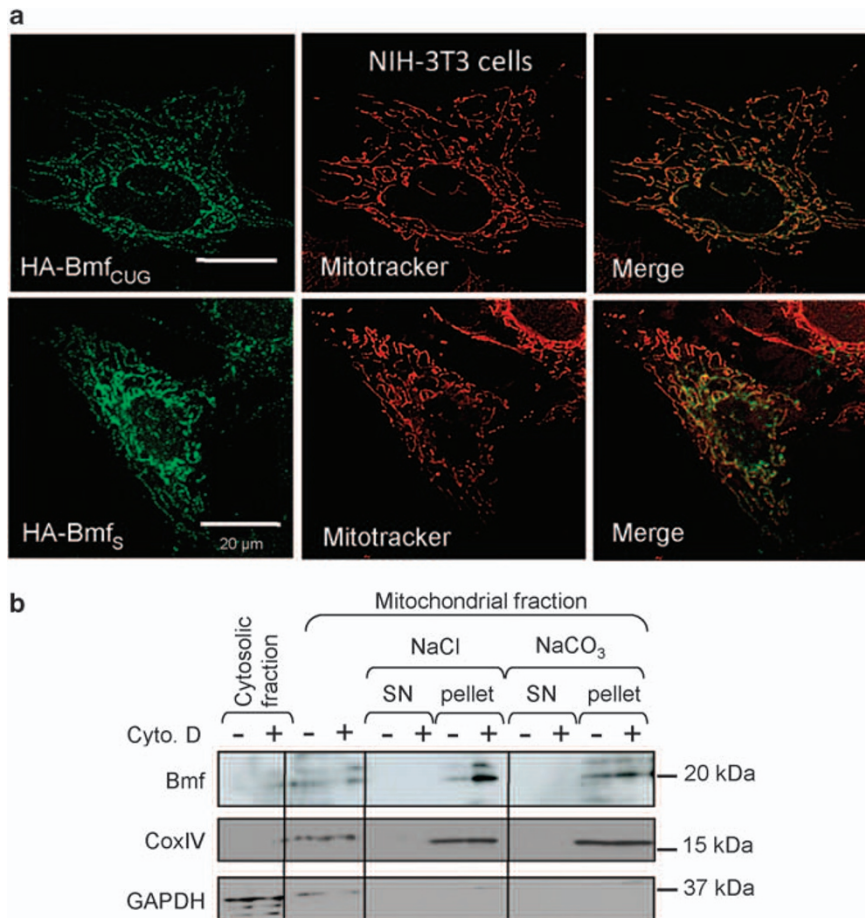


Figure 6 Bmf isoforms localize preferentially to the outer mitochondrial membrane. (a) NIH3T3 cells were transiently transfected with HA-tagged versions of Bmf_S or Bmf_{CUG}. Twenty-four hours after transfection, cells were fixed and prepared for immunofluorescence. (b) NIH3T3 cells were left untreated or cultured in the presence of 2 μ M cytochalasin D for 16 h. Cells were harvested, washed in PBS and lysed before subcellular fractionation and alkaline stripping of the mitochondria. Pellet and supernatant (SN) fractions were separated by SDS-PAGE, transferred onto nitrocellulose membranes and subjected to immunoblotting using anti-Bmf mAb (17A9). Membranes were reprobed with antibodies specific for the mitochondrial transmembrane protein CoxIV or cytoplasmic GAPDH

translated from the uncapped mRNA, but surprisingly, we also detected a second signal resembling Bmf_{CUG} (Figure 7c).

Accumulation of the Bmf protein and Bmf-dependent apoptosis upon inhibition of CAP-dependent translation. We investigated whether the Bmf protein can be induced under conditions that favor CAP-independent and, hence, IRES-mediated protein translation. To test this, we deprived NIH3T3 cells and HC11 mammary epithelial cells of serum or exposed them to hypoxia, both conditions known to favor CAP-independent translation.²¹ Furthermore, CAP-dependent translation was compromised by inhibition of the PI3K/AKT pathway or mTOR using LY294002 or rapamycin, respectively.²² Finally, we directly interfered with conventional translation using 4EGI-1, an inhibitor of the eukaryotic initiation factor (eIF) 4E–eIF4G interaction.²³ Notably, all these stimuli caused accumulation of both Bmf isoforms, whereas treatment of cells with the ER stressor tunicamycin, the DNA-damaging drug etoposide or the pan-kinase inhibitor staurosporine had no such effect (Figure 8a; not shown). Notably, treatment of both cell types with the

actin-depolymerizing agent cytochalasin D also led to an increase in Bmf protein levels (Figure 8a; Supplementary Figure 1d).

To evaluate whether Bmf is also important for cell death induction under these conditions, apoptosis was quantified in NIH3T3 cells stably expressing a short hairpin RNA (shRNA) targeting *bmf* mRNA for degradation by RNAi (Figure 8b). Consistent with a rate-limiting proapoptotic role of Bmf under these conditions, its knockdown rendered NIH3T3 cells refractory to cell death induced by stimuli that interfere with CAP-dependent translation, including serum deprivation or inhibition of the PI3K/AKT/mTOR network. Knockdown of Bmf also delayed cell death induced by cytochalasin D treatment, which does not associate with CAP-independent translation, but apoptosis induced by UV radiation, anoikis, the proteasome inhibitor Velcade or treatment with the histone deacetylase inhibitor Trichostatin A occurred normally (Figure 8b and Supplementary Figure 4).

We also investigated whether Bmf could be induced in SV40 MEF, which do not express significant levels of the Bmf protein, and whether the absence of the protein in *bmf*^{-/-} MEF could confer resistance to apoptosis induction.

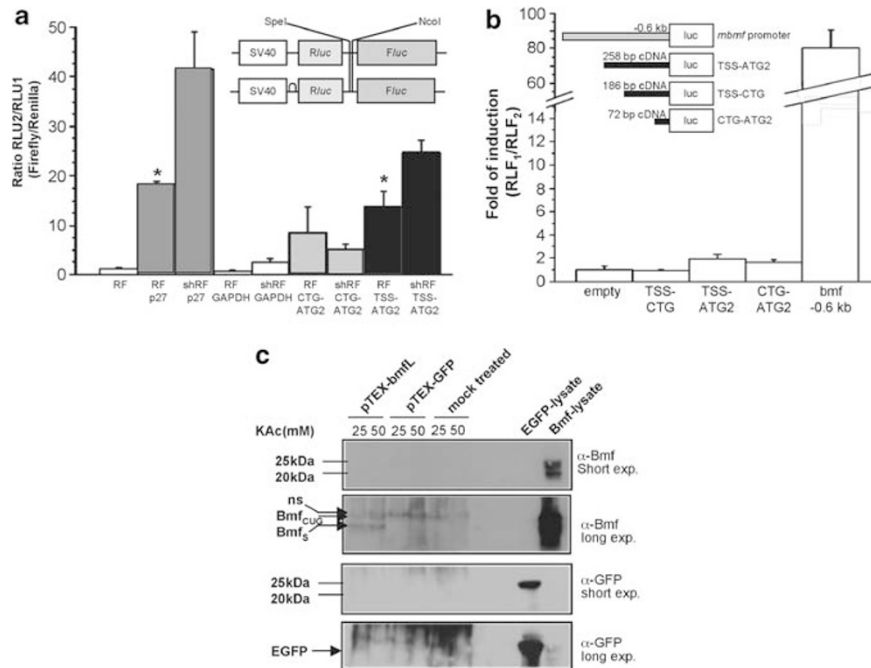


Figure 7 Bmf isoforms can be translated in a CAP-independent manner. (a) Constructs containing a bicistronic mRNA encoding Renilla (RN) and Firefly (FF) luciferase, driven by the SV40 minimal promoter and spaced by mouse *bmf* cDNA elements from the predicted TSS to translation initiating ATG2 in exon 3, CTG in exon 2 to ATG2, or an unrelated sequence from the human *GAPDH* gene were transiently transfected into 293T cells. Twenty-four hours later, cells were lysed and the different luciferase activities quantified using a Dual-Luciferase Assay kit to calculate the ratio of FF/RN activities in the absence or presence of the putative IRES element and an inhibitory stem-loop structure 5' of the first cistron, shifting the balance to IRES-mediated translation of the second cistron. Bars represent means \pm S.E.M. of three independent experiments performed in quadruplicates. Asterisks (*) represent significant differences between RF and shRF constructs ($P < 0.05$). (b) To exclude residual promoter activity in the putative IRES element, the indicated mouse *bmf* cDNA-derived sequences were subcloned into a promoter-less luciferase expression plasmid. After transient transfection into 293T cells, luciferase activity was quantified as described above and normalized to co-transfected RN luciferase. A 600 bp element from the *bmf* promoter served as positive control. One representative experiment performed in triplicate is shown. (c) cDNAs encoding mouse *bmf_L* or *GFP* were subcloned into the pTEX-polyA plasmid that contains a polyA tail 3' of the multiple cloning site and a 5' SP6 promoter for *in vitro* transcription. Uncapped mRNA was then used in a standard *in vitro* translation in reticulocyte lysates. Aliquots of the reactions were separated by SDS-PAGE along with protein lysates containing Bmf isoforms or GFP as a control (ns = nonspecific). Immunoblotting analysis was performed using anti-Bmf mAb (17A9) and anti-GFP mAb (Sigma-Aldrich)

Serum-deprived wt MEF and cells treated with inhibitors of the PI3K/AKT/mTOR network all induced the Bmf protein. When wt MEF were first serum deprived for 24 h, triggering Bmf accumulation, subsequent exposure to cycloheximide prevented further protein accumulation more potently than did inhibition of transcription with actinomycin D (Figure 9a). Similar observations were made in MEF treated with rapamycin or LY294002 (Figure 9b). Taken together, these observations again supported the idea that inhibition of CAP-dependent translation favors Bmf protein accumulation under these conditions, at least in part by IRES-mediated translation. Consistently, inhibition of the PI3K/AKT/mTOR network by LY294002 or rapamycin triggered cell death in *bmf*^{-/-} MEF less effectively. Notably, these cells still succumbed to apoptosis equally fast or even faster upon treatment with staurosporine (Figure 9c). Serum deprivation yielded inconsistent results in the different SV40 MEF clones tested, and the observed differences did not show statistically significant differences (Figure 9c), suggesting that some of the observed effects are cell type specific or depend on the type of immortalization.

As viral infection often associates with the inhibition of CAP-dependent translation, we speculated whether the loss of Bmf prevents attrition of T cells observed to occur early in such antiviral immune responses.²⁴ This situation can be mimicked

to a certain degree by injection of polyIC that triggers the type I IFN-dependent apoptotic loss of CD8⁺ T cells early in an immune response.²⁴ Therefore, wt and *bmf*^{-/-} mice were injected with a single dose of polyIC and the percentage of CD8⁺ T cells was quantified 20 h later. CD8⁺ T cell numbers declined but naive CD8⁺ CD44⁻ T cells were most affected by polyIC treatment in wt animals. In contrast, in mice lacking Bmf that presented with an overall reduced percentage of naive T cells, polyIC treatment had no such effect (Figure 9d).

Discussion

To provide a cell with the biggest possible flexibility to respond to highly diverse forms of stress, multiple modes of regulation are usually required to control the activation and function of individual BH3-only proteins. Protein-protein interaction, for example, with motor complex-associated proteins such as DLC molecules can lead to distinct subcellular localization of Bim or Bmf, at least in some cell types.⁸ Alternative splicing as a means of regulation has been described not only for Puma²⁵ and Bim²⁶ but also for Bmf.¹² However, none of the major isoforms of Bmf described in this study is generated by differential splicing but by different start-site usage and, therefore, do not represent equivalents of human BMF II or BMF III, found in CLL cells.¹² BMF II and BMF III, as well as

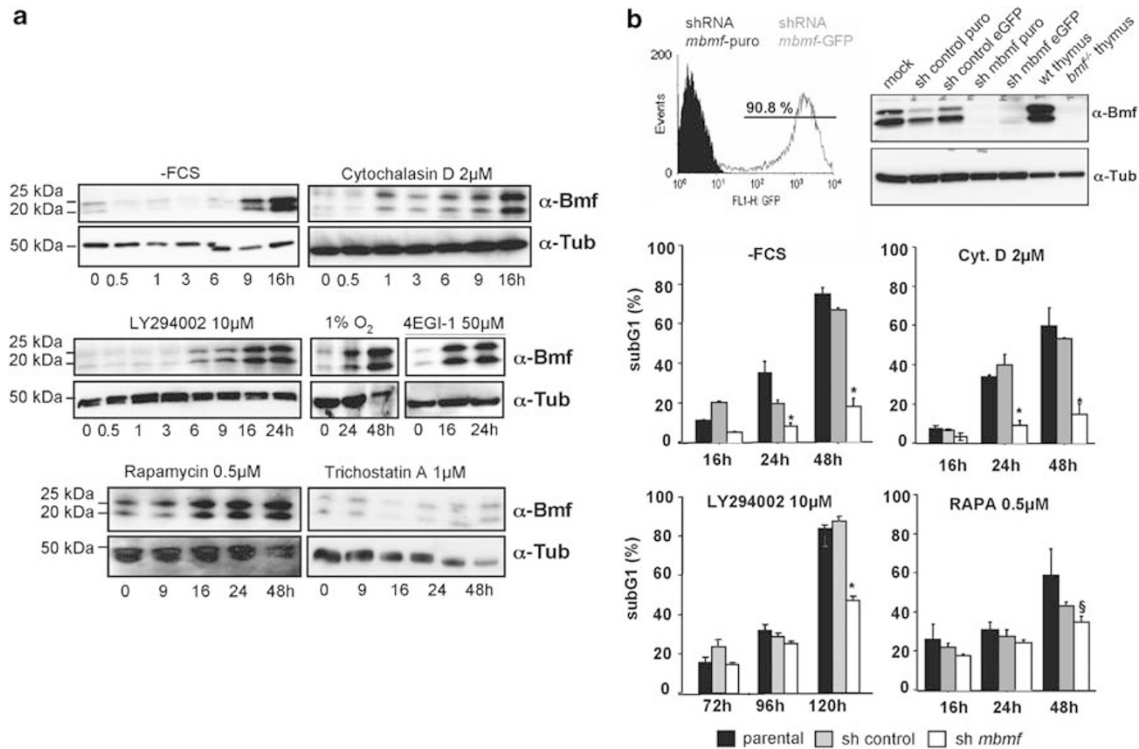


Figure 8 Bmf accumulates prior cell death in NIH3T3 cells. (a) NIH-3T3 fibroblasts deprived of serum or cultured in the presence of the indicated stimuli and concentrations over time. Cell extracts were separated by SDS-PAGE and immunoblotting was performed using the Bmf-specific mAb (17A9). Membranes were reprobbed with an anti-tubulin antibody to compare protein loading. (b) NIH3T3s were lentivirally transduced with shRNA targeting human (sh control) or mouse *bmf*. Transduction and knockdown efficiency was confirmed by flow-cytometric analysis and western blotting. Stable knockdown clones were selected using puromycin and used for survival analysis. Cells were deprived of serum or exposed to the indicated drugs. Apoptosis was quantified by sub-G1 staining of cells, followed by flow-cytometric analysis. Bars represent means \pm S.E. of three independent experiments performed in duplicates using two independent sh-clones. (*) indicates statistically significant differences between parental, sh_control and sh_ *bmf* expressing cells and (§) indicates significant differences between parental- and sh_ *bmf*-expressing cells ($P < 0.037$ for -FCS; $P < 0.002$ for Cyt. D; $P < 0.0019$ for LY294002; $P < 0.05$ for rapamycin)

the γ - and δ -isoforms of Puma, do lack a functional BH3 domain²⁵ and their physiological functions remains unclear. In contrast, all Bmf isoforms detected in our study could be coimmunoprecipitated together with Bcl-2 from lymphocytes, indicating that they must all contain a functional BH3 domain (Supplementary Figure 1b).

Functional analysis failed to show any differences in the binding pattern of Bmf isoforms to prosurvival Bcl-2 proteins, similar to observations made using alternatively spliced isoforms of Bim.²⁶ Bmf_{CUG} bound to Bcl-2, Bcl-x, Bcl-w and Mcl-1, as initially also reported for Bmf_S,¹⁵ but neither isoform bound effectively to the viral Bcl-2-like proteins BHRF1 or KS-Bcl-2 in our overexpression studies (Figure 3). Although Biacore analysis defined a low affinity of the Bmf BH3 domain for Mcl-1,²⁷ this interaction can be readily detected under conditions of overexpression (Figure 3; Puthalakath *et al.*¹⁵). Recently, we also observed interaction of endogenous Bmf with endogenous Mcl-1 in mouse B lymphoma cells (AV, unpublished), suggesting that the use of BH3-domain peptides cannot entirely recapitulate the interaction behavior of the full-length protein.

Similar to the major Bim isoforms, Bmf_S appeared somewhat more potent in reducing the colony-forming potential of MEF; however, this effect was not observed in U2OS cells. Both isoforms can engage Bax and Bak to promote cell killing, but Bmf_S seems to have a preference

for Bax (Figure 5). To our surprise, we observed that MEF lacking Bax and Bak showed reduced colony formation, most pronounced when both isoforms were overexpressed from a single transcript and at the moment, we can only speculate that these cells may either activate Bok under these conditions or die by necroptosis.¹⁹

Our observation that the generation of Bmf_{CUG} involves translation initiation from a CUG, encoded in exon 2 suggested that IRES-mediated translation might serve as a mechanism to initiate translation. This possible feature was overlooked initially when the short isoform of Bmf was first described.¹⁵ Our follow-up analysis suggests that both major isoforms actually appear to be translated in an IRES-dependent manner from alternative start sites contained in the *bmf* mRNA (Figures 2 and 7). Alternative start-site usage has also been reported for Bad, leading to the expression of two main isoforms, but ATG serves for initiation of translation in both cases.²⁸

During apoptosis, eIFs are modified early on, for example, by dephosphorylation of 4E-BP1 and subsequent caspase cleavage of eIF4G, both enforcing CAP-independent translation.²¹ Consistently, a number of apoptosis regulators including p53, Bcl-2, Apaf-1 and XIAP were reportedly generated from IRES elements under conditions of stress.²⁹ However, some of these proposed IRES elements were subsequently proven to be false and the activity observed in dual reporter

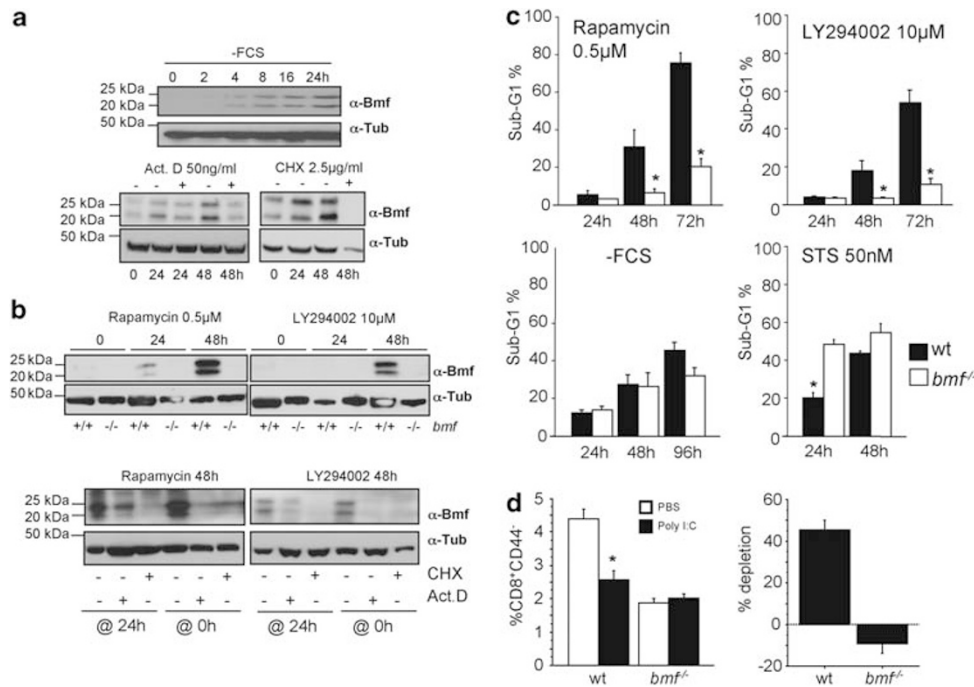


Figure 9 Bmf-deficiency delays apoptosis by cell stress associated with CAP-independent translation. (a) SV40 MEFs were deprived of serum in the absence or presence of actinomycin D or cycloheximide. Protein lysates were generated at the indicated time points and Bmf expression was analyzed by immunoblotting. (b) Wt or *bmf*^{-/-} SV40 MEFs were exposed to rapamycin or LY294002 up to 48 h (upper panel). Alternatively, actinomycin D or cycloheximide was added at *t* = 0 h or after 24 h of incubation with rapamycin or LY294002 (lower panel). (c) Cells lacking or expressing Bmf were treated with the indicated compounds over time. Apoptosis of MEF was assessed by sub-G1 staining and flow-cytometric analysis. Bars represent means ± S.E. of three independent experiments. Experiments using three independent MEF clones of each genotype yielded comparable results and were therefore pooled (STS = staurosporine). Asterisks (*) indicate statistically significant differences between wt and *bmf*^{-/-} MEF (*P* < 0.006 for LY294002; *P* < 0.001 for rapamycin). (d) Wt- and Bmf-deficient mice were injected i.p. with a single dose of polyI:C (100 μg per mouse) or saline. After 20 h, mice were killed and the percentage of naive CD8⁺CD44⁻ T cells in spleen quantified by flow-cytometric analysis. Bars represent means ± S.E.M. of three animals per genotype and group. (*) indicates statistically significant differences between wt and *bmf*^{-/-} (*P* < 0.003)

systems due to cryptic splicing events generating a 3'cistron of the second reporter.^{30–32} To strengthen our claim that Bmf can be translated in an IRES-mediated manner, we have (1) excluded residual promoter activity in the DNA sequences tested, (2) demonstrated that insertion of a hair-pin structure favors expression of the second cistron in dual reporter assays and, most importantly, performed (3) sequential transcription translation reaction using uncapped mRNA that confirmed translation of the Bmf protein in the absence of a 5'CAP structure (Figure 7). Consistently, endogenous Bmf expression was clearly induced by different stimuli that associate with the repression of CAP-dependent translation (Figures 8 and 9). The latter observation proposes a role for Bmf isoforms as sentinels that become activated in response to stress that associates with reprogramming of the translation machinery from CAP-dependent to CAP-independent translation, such as growth factor deprivation, hypoxia or inhibition of the PI3K/AKT/mTOR signaling axis (Figures 8 and 9; Supplementary Figure 1). Consistent with a role for Bmf as a sensor of this type of stress, knockdown or absence of Bmf interfered but ultimately failed to prevent apoptosis in response to some of the tested stimuli, suggesting that it must still collaborate with other cell death regulators. Whether Bmf also has a rate-limiting role for apoptosis induced upon physiological triggers of CAP-independent translation *in vivo*, such as viral infection or hypoxia, and whether the additional 24 aa in Bmf_{CUG} serve as an interface for protein–protein

interactions outside the Bcl-2 family will be subject of our future investigations.

Materials and Methods

Cell culture, primary cells and reagents. All cells were cultured at 37°C in a humidified atmosphere containing 5% CO₂. MEFs were isolated from E14.5 embryos after removal of the internal organs, brain and fetal liver by trypsin digestion of the remaining carcass. All experiments were performed using MEFs that were immortalized with the SV40 large T antigen. U2OS cells, MEFs and NIH3T3 murine fibroblasts were cultured in the DME medium supplemented with 10% fetal calf serum (FCS) (PAA, Vienna, Austria), 250 μM L-glutamine (Invitrogen, Vienna, Austria) and penicillin/streptomycin (1 Units/ml, Sigma-Aldrich, Vienna, Austria). IL3-dependent BaF3 pro-B lymphoid cells were cultured in RPMI 1640 medium, supplemented with 250 μM L-glutamine, 50 μM 2-mercaptoethanol, penicillin/streptomycin (1 Units/ml) and 10% FCS, supplemented with 15% of WEHI-3B cell supernatant. HC11 mouse mammary epithelial cells were cultured in RPMI 1640 medium, supplemented with 5 μg/ml bovine insulin (Sigma-Aldrich), 10 ng/ml murine EGF (Peprotec, London, UK), 250 μM L-glutamine, 50 μM 2-mercaptoethanol, penicillin/streptomycin (1 Units/ml) and 10% FCS. The generation of vav-bcl-2 transgenic³³ and *bmf*^{-/-} mice has been described previously.¹⁰

Apoptosis induction, sub-G1 and Annexin-V/propidium iodide staining. For induction of cell death, the following reagents were used: 2 μM Cytochalasin D (Sigma-Aldrich), 10 μM LY294002 (InvivoGen, San Diego, CA, USA), 500 nM rapamycin (Alexis, Lausen, CH, Switzerland), 50 μM 4EGI-1 (Alexis), 50 nM Staurosporine (Sigma-Aldrich) and 1 μg/ml Tunicamycin (Sigma-Aldrich). Cells cultured under hypoxic conditions were cultured in a humidified atmosphere containing 1% O₂.

For sub-G1 analysis, cells were collected, along with their supernatant, centrifuged for 5 min at 1500 r.p.m., 4°C. The pellet was then washed once with

PBS and centrifuged again. After supernatant removal, the pellet was resuspended in 500 μ l 70% methanol (in PBS) and fixed at -20°C . Cells were then washed with PBS and centrifuged for 5 min at 3000 r.p.m., 4°C . The pellet was resuspended in 475 μ l PBS with RNaseA (Sigma-Aldrich; final concentration 10 $\mu\text{g}/\text{ml}$) and incubated at 37°C for 20 min. Thereafter, 25 μ l of propidium iodide (final concentration 2 $\mu\text{g}/\text{ml}$) was added to the cell suspension, which was incubated for 10 min at 4°C before analysis in the flow cytometer, FACScan (Becton Dickinson, Vienna, Austria). Alternatively, the percentage of viable cells in culture was determined by staining them with 2 $\mu\text{g}/\text{ml}$ propidium iodide plus APC- or FITC-coupled Annexin-V in Annexin-binding buffer (Becton Dickinson) and subsequent flow-cytometric analysis.

Individual IVTT. cDNA encoding mbmf_L or GFP cDNA was subcloned in the pTEX plasmid containing a polyA sequence downstream of the multiple cloning site. DNA was linearized with NotI, run on a 1.5% agarose TAE gel and then purified using a gel extraction kit (Qiagen, Hilden, Germany). IVT using 25% volume of eluted DNA was performed using the SP6 MEGAScript Kit (Ambion, Brunn, Austria). RNA was recovered by LiCl precipitation (final concentration 4.5 M). RNA concentration was quantified in a spectrophotometer and 1 μg of *in vitro* transcribed RNA was subsequently translated using the Retic Lysate IVT kit (Ambion) according to the manufacturer's recommendation, in 25 or 50 mM potassium acetate containing reaction buffer. Protein was precipitated using 12% TCA and resuspended in $2 \times$ Laemmli buffer and separated by SDS-PAGE before immunoblotting.

Coupled IVTT reaction. Usually, 1 μ l plasmid DNA (100 ng) was mixed with 10 μ l translation mix containing reticulocyte extract and, optional, 1 μ l ^{35}S methionine (Amersham, Vienna, Austria). Samples were incubated for 90 min at 30°C and then frozen until SDS-PAGE was performed.

SDS-PAGE: In all, 3 μ l of each sample was diluted in ONYX lysis buffer, mixed 1:3 with the Laemmli loading buffer and applied on a 14–20% precast gradient polyacrylamide gel. On one lane, a protein size marker was loaded. Electrophoresis was performed at 70 V in Tris-Glycine buffer. After electrophoresis, the gel was vacuum dried and exposed to an X-ray film for 2 days. Results were obtained after developing the film using AGFA Curix 60 (Vienna, Austria) photo imager. Alternatively, nonradioactive reactions were electroblotted onto nitrocellulose membranes and subjected to immunoblotting using anti-Bmf mAb 17A9.

Transient transfections, immunoblotting, immunoprecipitation and phosphatase treatment. 293T human embryonic kidney cells or NIH3T3 fibroblasts were transiently transfected in 6-well plates using 3 μ l of Lipofectamine 2000 reagent (Invitrogen) and a total of 1 μg of plasmid DNA. Cells were incubated in Optimum (Gibco, Invitrogen) with the transfection mix for 6 h before replacing the medium. After 48 h, cells were harvested and lysed in ONYX buffer (20 mM Tris-HCl, pH 7.5, 135 mM NaCl, 1.5 mM MgCl_2 , 1 mM EGTA, 1 mM EDTA, 1% Triton X-100, 10% glycerol) for 30 min on ice. Insoluble debris was cleared by centrifugation and protein concentration was quantified using the Bradford assay. Usually, 75–100 μg of protein separated by SDS-PAGE using 4–20% PAGE Novex-ready gels (Invitrogen). After transfer, membranes were probed with rat monoclonal antibodies specific for Bmf (clone 9G10, 17A9 or 12E10) or specific for the FLAG epitope (mouse anti-FLAG M2, Sigma-Aldrich). Equal loading of proteins was confirmed by probing filters with antibodies specific for α -tubulin (DM1A, Santa Cruz Biotechnologies, Santa Cruz, CA, USA), GAPDH, 71.1 (Sigma-Aldrich) or rabbit anti-CoxIV polyclonal (Abcam, Cambridge, UK) for mitochondrial fractions. Horseradish peroxidase-conjugated sheep-anti-rat Ig antibodies (Silenus, Vienna, Austria) served as secondary reagents and the enhanced chemiluminescence system was used for detection. Immunoprecipitation was performed using Protein G-sepharose (GE Healthcare, Vienna, Austria). For dephosphorylation, single cell suspensions were prepared from the thymus or spleen from wt mice. Resuspended cells were washed twice in PBS and then lysed 30 min at 4°C in Chaps buffer (20 mM Tris-HCl, 5 mM MgCl_2 , 137 mM KCl, 1 mM EDTA, 1 mM EGTA, 0.5% Chaps, pH 7.5) supplemented with (Complete, Roche, Vienna, Austria). Cellular debris were removed by centrifugation at $10\,000 \times g$ for 20 min at 4°C . Protein extract was dephosphorylated with lambda protein phosphatase (7 Units/ μg of protein extract) (BioLabs, Vienna, Austria) and 2 mM MnCl_2 2 h at 4 or 30°C . The reaction was stopped by addition of SDS-PAGE loading buffer.

Luciferase assays. Lipofectamine was used to transiently transfect 293T cells with different dual-luciferase constructs for 6 h. After additional 24 h, cells were harvested

and RN and FF luciferase activity was quantified using the Dual-Luciferase Reporter Assay kit (Promega, Mannheim, Germany) according to the manufacturer's recommendation.

Immunofluorescence staining. Cells were cultured on glass coverslips, and 24 or 48 h after lipofectamine transfection, cultures were briefly washed with PBS and incubated for 30 min at 37°C with 100 nM MitoTracker Red CMXRos (Molecular Probes, Invitrogen, Austria) in culture medium to stain the mitochondria. Cultures were then briefly washed with PBS, the medium was removed and cells were fixed for 15 min at room temperature with 4% PFA (in PBS). Cells were then washed three times with PBS and further incubated for 1 h with PBS containing 0.1% Triton X-100, 1% bovine serum albumin and 10% FCS for permeabilization and blocking. Incubation with primary antibody (mouse anti-HA clone: 12CA5, Sigma-Aldrich, 1:100 in blocking solution) was performed overnight at 4°C . After further three washes with PBS, cells were incubated with secondary antibody (Alexa-fluor-488-labeled anti-mouse, Molecular Probes, Invitrogen; 1:100 in blocking solution) for 1 h at room temperature, then washed three times again and incubated with DAPI (1 $\mu\text{g}/\text{ml}$, in PBS) for nuclear staining for 10 min at room temperature. Finally, after another washing step, cells were fixed with Vectashield antifade mounting medium (Vector Laboratories, Burlingame, CA, USA) and the glass coverslips were mounted on microscope slides. Cell images were collected with a confocal laser scanning microscope (Zeiss LSM 510 Axiovert 100 M, $63 \times /1.4$ oil immersion lens; Carl Zeiss Microimaging, Inc., Jena, Germany), with the resolution set at 1024×1024 pixels, and pinholes set to acquire images of below 1 μm thickness. Further image processing, such as background correction, adjustment of brightness and contrast and export to tif format, were made using ImageJ software (<http://rsbweb.nih.gov/ij/>).

For fluorescence detection of IRES-mediated expression of YFP 293T, HEK cells cultured on glass coverslips were transfected with plasmid constructs containing cDNA encoding a ECFP-Venus fusion protein, or a sequence in which both ORFs were separated by the putative Bmf-IRES, and were then exposed to 50 μM 4EGI-1, 0.5 μM rapamycin for 24 h or were left untreated. Next, cells were fixed with 4% PFA in PBS at room temperature, washed three times with PBS and mounted on microscope slides with the Vectashield antifade mounting medium. Images were then acquired using a Leica SP5 confocal laser scanning microscope (Leica Microsystems, Wetzlar, Germany) with a $\times 63$ glycerol immersion objective, applying the LAS AF acquisition software version 2.1.0 (Leica Microsystems, Wetzlar, Germany). Cells were alternately excited either with the 458 nm or the 514 nm laser line of an Argon laser and emission filter sliders were set to 460–495 nm or to 520–590 nm to detect CFP and YFP, respectively. Image resolution was set at 512×512 pixels and pinholes to 1 Airy unit. Relative emission intensities of acquired images were finally quantified using the ImageJ software.

Mitochondrial subfractionation. After 16 h of incubation with 2 μM Cytochalasin D or solvent control, NIH3T3 cells were harvested in 300 μ l of isotonic mitochondrial buffer (MB) (70 mM sucrose, 210 mM mannitol, 1 mM EDTA, 10 mM Hepes, pH 7.5) supplemented with proteases inhibitor cocktail (Complete, Roche). Cells were left for 15 min on ice and then they were broken by 7 passages repeated for 3 times through a 25-G needle fitted on a 1 ml syringe. Cell were suspended and then centrifuged at $2000 \times g$ at 4°C for 5 min to remove unbroken cells. Lysates were spun further for 10 min at $13\,000 g$ at 4°C to pellet the mitochondria, ER and nuclei. The cytosolic supernatant fraction was subsequently centrifuged for 1 h at 4°C at 39 000 r.p.m. in an ultracentrifuge. Supernatant was then precipitated with 12% TCA and resuspended in 45 μ l of $2 \times$ Laemmli buffer before boiling (5 min, 95°C). The 13 K pellet = heavy membrane fraction was resuspended in 65 μ l MB-EGTA buffer (containing 0.5 mM EGTA instead of EDTA) and further centrifuged at $500 \times g$ for 3 min at 4°C to separate the nuclear fraction. The supernatant containing the mitochondria was subdivided into 3 aliquots and centrifuged at $10\,000 \times g$, for 10 min at 4°C . The pellet resulting from one aliquot was resuspended in 15 μ l of MB-EGTA buffer containing 1% Triton and used for protein quantification by Bradford. The two other mitochondrial pellets were subjected to alkali extraction. Pellets were resuspended in 125 μ l of H_2O and 125 μ l of NaCl (2 M) or Na_2CO_3 (2 M). Samples were incubated on ice for 30 min mixed by vortexing every 10 min, followed by centrifuged at $100\,000 \times g$ for 30 min at 4°C . Alkaline-sensitive fractions (supernatant) were precipitated adding 12% TCA (final concentration) and then resuspended in 15 μ l of $2 \times$ Laemmli buffer before boiling. The alkaline-resistant pellet fraction was boiled in the same volume. Finally, 15 μ l of each fraction was loaded on a 4–20% Tris-HCl gel (Bio-Rad) and separated by SDS gel electrophoresis.

Viral transduction and colony-formation assays. U2OS and NIH3T3 cells were transduced with lentiviruses encoding different isoforms of Bmf, MEF lacking Bax or Bak were transduced retrovirally.

For overexpression of the various Bmf isoforms, the corresponding cDNAs were PCR amplified and recombined into pDONR-207 (Invitrogen) using Invitrogen's B/P recombination kit. Sequence-verified clones were used for L/R recombination with pHR-tetCMV-dest,¹⁷ thereby generating the lentiviral plasmids pHR-tetCMV-Bmf_S, pHR-tetCMV-Bmf_{CUG}, pHR-tetCMV-Bmf_S/L/A, pHR-tetCMV-Bmf_{CUG}/L/A and pHR-tetCMV-eGFP. Generation of lentiviral plasmid for constitutive knockdown of human Bmf were described before.¹⁷ For the knockdown of mouse Bmf, 5'GATCCCCTCAGTCGACTCCAGCTCTTTTCAAGAGAAAGAGCTGGAGTCGACTGATTTTGGAA3' (sense) and 5'AGCTTTTCCAAAATCAGTCGACTCCAGCTCTTTCTCTTGA AAAGAGCTGGAGTCGACTGAGGG3' (antisense) oligonucleotides were phosphorylated, annealed and cloned into the BglII-HindIII site of pENTR-THT.¹⁷ Thereafter, sequence-verified clones were used for L/R recombination into the final lentiviral destination vectors pHR-dest-SFFV-eGFP and pHR-dest-SFFV-Puro, thereby generating pHR-THT-mBmf shRNA-SFFV-eGFP and pHR-THT-mBmf shRNA-SFFV-Puro.

For lentiviral transfection, human HEK 293T cells were transiently transfected with lentiviral plasmids containing cDNAs coding for mouse Bmf_S, Bmf_{CUG}, Bmf_S/L/A mutant, Bmf_{CUG}/L/A mutant or eGFP as control, along with the packaging plasmids pSPAX and pVSV-G. After 48 and 72 h, lentiviral supernatant was collected and sterile filtered (0.2 μM), supplemented with Polybrene to a final concentration of 4 μg/ml and added to the target cells overnight.

For retroviral transduction of MEF, Lipofectamine (Invitrogen) was used to transiently transfect Phoenix packaging cells with constructs encoding for Bmf_S, Bmf_{CUG}, both isoforms, or empty control subcloned in the retroviral pBabe-puro backbone. After 48 h, supernatant was collected and 0.20 μm filter sterilized. Polybrene was then added to reach a final concentration of 4 μg/ml. The viral supernatant was added to MEF lacking Bax or Bak by spin infection. The next morning, fresh medium was added to the infected cells. After 48 h, the medium was replaced by a medium containing 2 μg/ml puromycin. Selection was performed for 1 week during which the medium was changed twice.

For assessment of colony formation, cells were washed once with PBS and incubated for 10 min in 0.5 ml of crystal violet staining solution (0.2% crystal violet in 50% methanol). Plates were then rinsed three times with bi-distilled water, air-dried and stored in the dark until photographic documentation.

Statistical analysis. Statistical analysis was performed using the unpaired Student *t*-test and a Stat-view 4.1 software program (SAS Institute, Cary, NC, USA). *P*-values of <0.05 were considered to indicate statistically significant differences.

Conflict of interest

The authors declare no conflict of interest.

Acknowledgements. We thank Professors A Strasser, C Borner, M Schuler and W Doppler for cells and reagents; S Kiessling and F Müllauer for first experiments initiating this work; W Chmielewski for help with MEF experiments; B Tomaselli for help with hypoxia experiments; Irene Gaggl for expert technical assistance, as well as all our colleagues in the lab for insightful discussions. This work was supported by grants from the AICR, St. Andrews, UK (no. 06-0440), the Graduate School for Molecular Biology and Oncology (MCBO) and the SFB021, both funded by the Austrian Science Fund (FWF).

1. Giam M, Huang DC, Bouillet P. BH3-only proteins and their roles in programmed cell death. *Oncogene* 2008; **27** (Suppl 1): S128–S136.
2. Jeffers JR, Parganas E, Lee Y, Yang C, Wang J, Brennan J *et al*. Puma is an essential mediator of p53-dependent and -independent apoptotic pathways. *Cancer Cell* 2003; **4**: 321–328.
3. Villunger A, Michalak EM, Coultas L, Mullauer F, Bock G, Ausserlechner MJ *et al*. p53- and drug-induced apoptotic responses mediated by BH3-only proteins puma and noxa. *Science* 2003; **302**: 1036–1038.
4. Jost PJ, Grabow S, Gray D, McKenzie MD, Nachbur U, Huang DC *et al*. XIAP discriminates between type I and type II FAS-induced apoptosis. *Nature* 2009; **460**: 1035–1039.

5. Yin X-M, Wang K, Gross A, Zhao Y, Zinkel S, Klocke B *et al*. Bid-deficient mice are resistant to Fas-induced hepatocellular apoptosis. *Nature* 1999; **400**: 886–891.
6. Bouillet P, Purton JF, Godfrey DI, Zhang L-C, Coultas L, Puthalakath H *et al*. BH3-only Bcl-2 family member Bim is required for apoptosis of autoreactive thymocytes. *Nature* 2002; **415**: 922–926.
7. Egle A, Harris AW, Bouillet P, Cory S. Bim is a suppressor of Myc-induced mouse B cell leukemia. *PNAS* 2004; **101**: 6164–6169.
8. Pinon JD, Labi V, Egle A, Villunger A. Bim and Bmf in tissue homeostasis and malignant disease. *Oncogene* 2008; **27** (Suppl 1): S41–S52.
9. Puthalakath H, Strasser A, Huang DCS. Rapid selection against truncation mutants in yeast reverse two-hybrid screens. *BioTechniques* 2001; **30**: 984–988.
10. Labi V, Erlacher M, Kiessling S, Manz C, Frenzel A, O'Reilly L *et al*. Loss of the BH3-only protein Bmf impairs B cell homeostasis and accelerates gamma irradiation-induced thymic lymphoma development. *J Exp Med* 2008; **205**: 641–655.
11. Villunger A, Scott C, Bouillet P, Strasser A. Essential role for the BH3-only protein Bim but redundant roles for Bax, Bcl-2, and Bcl-w in the control of granulocyte survival. *Blood* 2003; **101**: 2393–2400.
12. Morales AA, Olsson A, Celsing F, Osterborg A, Jondal M, Osorio LM. Expression and transcriptional regulation of functionally distinct Bmf isoforms in B-chronic lymphocytic leukemia cells. *Leukemia* 2004; **18**: 41–47.
13. Frenzel A, Labi V, Chmielewski W, Ploner C, Geley S, Fiegl H *et al*. Suppression of B-cell lymphomagenesis by the BH3-only proteins Bmf and Bad. *Blood* 2010; **115**: 995–1005.
14. Hitomi J, Christofferson DE, Ng A, Yao J, Degterev A, Xavier RJ *et al*. Identification of a molecular signaling network that regulates a cellular necrotic cell death pathway. *Cell* 2008; **135**: 1311–1323.
15. Puthalakath H, Villunger A, O'Reilly LA, Beaumont JG, Coultas L, Cheney RE *et al*. Bmf: a pro-apoptotic BH3-only protein regulated by interaction with the myosin V actin motor complex, activated by anoikis. *Science* 2001; **293**: 1829–1832.
16. Mackus WJ, Kater AP, Grummels A, Evers LM, Hooijbrink B, Kramer MH *et al*. Chronic lymphocytic leukemia cells display p53-dependent drug-induced Puma upregulation. *Leukemia* 2005; **19**: 427–434.
17. Ploner C, Rainer J, Niederegger H, Eduardoff M, Villunger A, Geley S *et al*. The BCL2 rheostat in glucocorticoid-induced apoptosis of acute lymphoblastic leukemia. *Leukemia* 2008; **22**: 370–377.
18. Weber A, Paschen SA, Heger K, Wilfling F, Frankenberg T, Bauerschmitt H *et al*. BimS-induced apoptosis requires mitochondrial localization but not interaction with anti-apoptotic Bcl-2 proteins. *J Cell Biol* 2007; **177**: 625–636.
19. Touriol C, Bornes S, Bonnafant S, Audigier S, Prats H, Prats AC *et al*. Generation of protein isoform diversity by alternative initiation of translation at non-AUG codons. *Biol Cell* 2003; **95**: 169–178.
20. Kullmann M, Gopfert U, Siewe B, Hengst L. ELAV/Hu proteins inhibit p27 translation via an IRES element in the p27 5'UTR. *Genes Dev* 2002; **16**: 3087–3099.
21. Spriggs KA, Stoneley M, Bushell M, Willis AE. Re-programming of translation following cell stress allows IRES-mediated translation to predominate. *Biol Cell* 2008; **100**: 27–38.
22. Wang X, Proud CG. The mTOR pathway in the control of protein synthesis. *Physiology* 2006; **21**: 362–369.
23. Moerke NJ, Aktas H, Chen H, Cantel S, Reibarkh MY, Fahmy A *et al*. Small-molecule inhibition of the interaction between the translation initiation factors eIF4E and eIF4G. *Cell* 2007; **128**: 257–267.
24. Bahl K, Kim SK, Calcagno C, Ghersi D, Puzone R, Celada F *et al*. IFN-induced attrition of CD8 T cells in the presence or absence of cognate antigen during the early stages of viral infections. *J Immunol* 2006; **176**: 4284–4295.
25. Nakano K, Vousden KH. PUMA, a novel proapoptotic gene, is induced by p53. *Mol Cell* 2001; **7**: 683–694.
26. O'Connor L, Strasser A, O'Reilly LA, Hausmann G, Adams JM, Cory S *et al*. Bim: a novel member of the Bcl-2 family that promotes apoptosis. *EMBO J* 1998; **17**: 384–395.
27. Chen L, Willis SN, Wei A, Smith BJ, Fletcher JL, Hinds MG *et al*. Differential targeting of prosurvival Bcl-2 proteins by their BH3-only ligands allows complementary apoptotic function. *Mol Cell* 2005; **17**: 393–403.
28. Ranger AM, Zha J, Harada H, Datta SR, Danial NN, Gilmore AP *et al*. Bad-deficient mice develop diffuse large B cell lymphoma. *PNAS* 2003; **100**: 9324–9329.
29. Graber TE, Holcik M. Cap-independent regulation of gene expression in apoptosis. *Mol Biosyst* 2007; **3**: 825–834.
30. Kozak M. A second look at cellular mRNA sequences said to function as internal ribosome entry sites. *Nucleic Acids Res* 2005; **33**: 6593–6602.
31. Baranick BT, Lemp NA, Nagashima J, Hiraoka K, Kasahara N, Logg CR. Splicing mediates the activity of four putative cellular internal ribosome entry sites. *PNAS* 2008; **105**: 4733–4738.
32. Saffran HA, Smiley JR. The XIAP IRES activates 3' cistron expression by inducing production of monocistronic mRNA in the {beta}gal/CAT bicistronic reporter system. *RNA* 2009; **15**: 1980–1985.
33. Ogilvy S, Metcalf D, Print CG, Bath ML, Harris AW, Adams JM. Constitutive bcl-2 expression throughout the hematopoietic compartment affects multiple lineages and enhances progenitor cell survival. *PNAS* 1999; **96**: 14943–14948.

Supplementary Information accompanies the paper on Cell Death and Differentiation website (<http://www.nature.com/cdd>)